Ultimate strength of longitudinally stiffenend plate girders under combined loads

Autor(en): **Ostapenko, A. / Chern, C.**

Objekttyp: **Article**

Zeitschrift: **IABSE reports of the working commissions = Rapports des commissions de travail AIPC = IVBH Berichte der Arbeitskommissionen**

Band (Jahr): **11 (1971)**

PDF erstellt am: **08.07.2024**

Persistenter Link: https://doi.org/10.5169/seals-12070

II

Ultimate Strength of Longitudinally Stiffened Plate Girders under Combined Loads

Résistance à la ruine des poutres à âme pleine cisaillées et fléchies, munies de raidisseurs longitudinaux

Traglast längsversteifter Blechträger unter Biegung und Querkraft

A. OSTAPENKO
Professor of Civil Engrg.
Lehigh University
Bethlehem, Pa., USA

C. CHERN
Assistant Prof. of Civil Engrg.
North Dakota State University
Fargo, N.D., USA

1. INTRODUCTION

Recognition of the fact that the web of plate girders possesses considerable post-buckling capacity led to research on their ultimate strength. Plate girders with transverse stiffeners (1) as well as girders with transverse and longitudinal stiffeners (5) were investigated. However, essentially all of this research dealt with symmetrical girders, that is, the centroidal axis was at the mid-depth. Since many plate girders are unsymmetrical, the authors developed a new ultimate strength method first for transversely stiffened girders (2,3,4,8). Then the method was extended to longitudinally stiffened girders (7). Besides handling unsymmetrical girders, this new theory gave not only the shear or bending strength, but also a continuous determination of the girder strength under any combination of shear and moment (7). Presented here is a brief description of the method and a comparison with some test results.

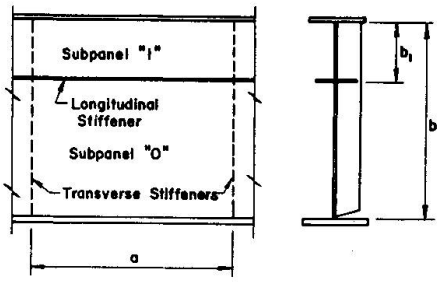

Figure 1

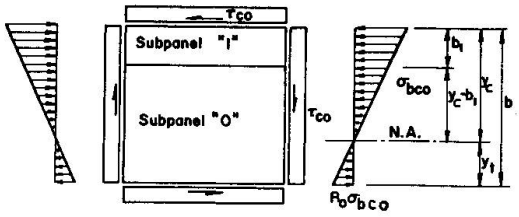

Figure 2

A plate girder panel subdivided by the longitudinal stiffener into two subpanels, subpanels "1" and "0", is shown in Fig. 1. The narrow subpanel "1" is subjected to shear and a linearly varying compression stress as shown in Fig. 2. The other subpanel (subpanel "0") is under shear and a normal stress varying linearly from compression to tension.

Deformation of a plate subpanel under shear is linear up to the point of buckling (γ_c). The shear in excess of the buckling value will be carried by the tension field action of the web (2). The shear strain at the

instant of reaching the ultimate load can be approximated by assuming that it corresponds to tensile yielding along the panel diagonal.

$$\gamma_u = \frac{\sigma_{yw}}{E} \left(\alpha + \frac{1}{\alpha}\right) \tag{1}$$

After this, the shear strain is assumed to increase at a constant average shear stress. For simplicity, the transition from the buckling strain to the ultimate strain may be assumed to be linear.

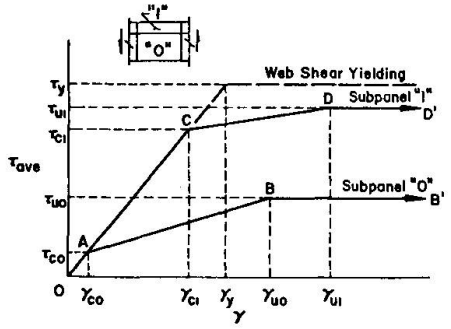

Figure 3

Consideration of the buckling and ultimate shear strains for each subpanel individually and the requirement of compatibility that the shear deformations in both subpanels be equal provide a means of defining the shear-deformation response of the whole web panel. The panel behaves like a beam until subpanel "0" reaches its buckling stress τ_{co}, indicated by point A in Fig. 3. From then on, subpanel "0" develops tension field action which produces a more rapid shear deformation as illustrated by line AB. Subpanel "1" remains flat and continues behaving linearly until it reaches its buckling stress at point C. Subpanel "0" has not yet attained its ultimate strength since the compatibility relationship of the subpanels indicates that $\gamma_{c1} < \gamma_{uo}$. After subpanel "1" buckles, the subpanels develop their ultimate strengths individually. The web shear forces at each stage of loading are obtained by multiplying the corresponding average shear stresses by the respective web subpanel areas.

When in addition to shear, bending stresses are acting on the subpanels as shown in Fig. 2, the web deformation pattern is analogous to that shown in Fig. 3, except that the critical buckling stresses τ_{co} and τ_{c1} are computed for a combined state of stress rather than for pure shear. It is assumed that the moment in excess of the moment which causes buckling of a subpanel web is carried only by the flanges, lontiduinal stiffener, and the unbuckled subpanel.

Stresses and forces that develop in the flanges and the longitudinal stiffener in the course of the deformation of the web panel may cause failure in one of them, thus precipitating failure of the whole panel. The following modes of failure may be possible: (a) shear failure of the web plate, (b) buckling or yielding of the compression flange, or (c) yielding of the tension flange. Failure of the longitudinal stiffener by lateral or torsional buckling may precede (a), (b) and (c), but it will usually only reduce rather than limit the panel capacity by changing the panel in effect from a longitudinally stiffened to a transversely stiffened one.

The applicable mode is determined by calculating the stresses in the flanges and the longitudinal stiffener at each significant loading level and checking them against the critical stresses. This way a continuous interaction curve is obtained.

A girder panel subjected to a particular combination of shear and moment is visualized to be a panel in a girder shown in Fig. 4a. The moment at the mid-panel is then defined in terms of the shear span ratio.

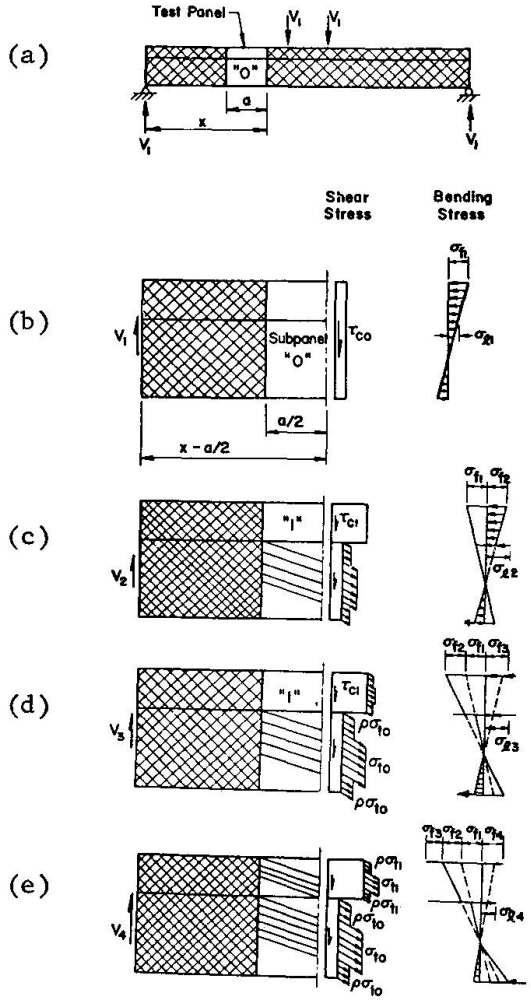

Figure 4

$$\mu = \frac{M}{bV} = \frac{x - a/2}{b} \tag{2a}$$

that is,
$$M = \mu\, bV \tag{2b}$$

2. REFERENCE STRESSES

Stresses in the flanges, stiffener, and the web subpanels are developed at various levels of loading by different mechanisms involving pre-buckling, post-buckling, and post-ultimate behavior of the individual panel components. The stresses at the transition from one mechanism to another are the reference stresses which provide a means of determining the mode of panel failure and the ultimate load.

Stresses at the Load Causing Buckling of Subpanel "0" - When subpanel "0" reaches the buckling stress τ_{co}, the total panel shearing force V_1 (Fig. 4b) is given by

$$V_1 = \tau_{co}\, A_w \tag{3}$$

where $A_w = bt$ = panel web area.

The stress at the web-to-longitudinal stiffener junction, $\sigma_{b_{co}}$, and at the bottom flange, $R_o\sigma_{b_{co}}$, can be obtained from the ordinary beam equations as a function of V_1 and thus of τ_{co} (see Fig. 2).

With this information, τ_{co} is computed from the following interaction equation of a plate subjected to a combination of shear and bending stresses (6).

$$\left(\frac{\tau_{co}}{\tau_{cro}}\right)^2 + \frac{1 + R_o}{2}\left(\frac{\sigma_{bco}}{\sigma_{cpo}}\right) + \frac{1 - R_o}{2}\left(\frac{\sigma_{bco}}{\sigma_{cpo}}\right)^2 = 1.0 \tag{4}$$

in which the buckling stresses for pure shear, τ_{cro}, and for pure bending, σ_{cpo}, are computed from

$$\tau_{cro} = k_{vo}\, \sigma_e \tag{5a}$$

$$\sigma_{cpo} = k_{bo}\, \sigma_e \tag{5b}$$

where $\sigma_e = [(\pi^2 E)/(12\,(1-\nu^2))]/\beta_o^2$.

The buckling coefficients k_{vo} and k_{bo} for a web plate assumed to be fixed at the horizontal edges and pinned at the vertical edges may be obtained from (4,7)

$$k_{vo} = \frac{5.34}{\alpha_o^2} + \frac{6.55}{\alpha_o} - 13.71 + 14.10\,\alpha_o \text{ , for } \alpha_o < 1.0 \tag{6a}$$

or

$$k_{vo} = 8.98 + \frac{6.18}{\alpha_o^2} - \frac{2.88}{\alpha_o^3}, \quad \text{for} \quad \alpha_o \geq 1.0 \tag{6b}$$

and

$$k_{bo} = 13.54 - 15.64\, R_o + 13.32\, R_o^2 + 3.38\, R_o^3 \tag{7}$$

where R_o is the ratio of the maximum tensile stress (or minimum compressive stress) to the maximum compressive stress for subpanel "0" under combined loads as shown in Fig. 2, and α_o and β_o are, respectively, the aspect ratio, $(a)/(b-b_1)$, and the slenderness ratio, $(b-b_1)/t$, of subpanel "0".

With τ_{co} thus computed, the buckling strength contributed by subpanel "0" alone is

$$V_{\tau o} = \tau_{co}\, A_{wo} \tag{8}$$

where $A_{wo} = (b-b_1)t$ is the web area of subpanel "0".

As shown in Fig. 4b, the stresses in the compression flange and in the longitudinal stiffener are, respectively,

$$\sigma_{f1} = \frac{V_1\, \mu b}{I}\, y_c \tag{9a}$$

and

$$\sigma_{\ell 1} = \frac{V_1\, \mu b}{I}\, (y_c - b_1) \tag{9b}$$

Stresses at the Load Causing Buckling of Subpanel "1" - Following the procedure described above for panel "0", the buckling shear of subpanel "1" is

$$V_{\tau 1} = \tau_{c1}\, A_{w1} \tag{10}$$

When $V_{\tau 1}$ is reached, the shear force carried by the whole panel web is

$$V_2 = V_{\tau o} + V_{\tau 1} + V_{\sigma o} \left(\frac{\gamma_{c1} - \gamma_{co}}{\gamma_{uo} - \gamma_{co}} \right) \tag{11}$$

where $V_{\sigma o}$ is the shear strength of subpanel "0" when the tension field action is fully developed (Eq. (14)), $\gamma_{co} = \tau_{co}/G$ and $\gamma_{c1} = \tau_{c1}/G$ are the strains of subpanels "0" and "1" corresponding to the web buckling stresses τ_{co} and τ_{c1} and γ_{uo} is the approximate shear strain when subpanel "0" reaches its ultimate load (it is obtained from Eq. (1) by substituting α_o for α).

The increments of stresses for the interval of the panel shear from V_1 to V_2 are, as shown in Fig. 4c

$$\sigma_{f2} = \frac{(V_2 - V_1)\, \mu b}{I}\, y_c \tag{12a}$$

and

$$\sigma_{\ell 2} = \frac{(V_2 - V_1)\, \mu b}{I}\, (y_c - b_1) + \frac{H_o'}{2A_{\ell s}} \tag{12b}$$

where

$$H'_o = V_{\sigma o}\left(\frac{\gamma_{c1} - \gamma_{co}}{\gamma_{uo} - \gamma_{co}}\right) \cot \varphi_{co} \tag{13}$$

is the horizontal component of the tension field force of subpanel "0" which must be carried by the longitudinal stiffener in addition to the stress contributed by the bending moment.

Stresses at the Load Developing the Post-Buckling Strength of Subpanel "0" - The stress distribution for this stage is shown in Fig. 4d. The strain condition is indicated in Fig. 3 by γ_{uo} and the tension field action of subpanel "1" has formed only partially.

The full tension field action contribution of subpanel "0" to the shear strength is given by

$$V_{\sigma o} = \frac{1}{2}\sigma_{to} A_{wo}\left[\sin 2\varphi_{co} - (1-\rho)\alpha_o + (1-\rho)\alpha_o \cos 2\varphi_{co}\right] \tag{14}$$

with σ_{to} from

$$\sigma_{to} = \sigma_{yw}\left(D_o + \sqrt{1 + B_o - C_o^2 + D_o^2}\right) \tag{15}$$

where

$$B_o = 3\sqrt{C_o^2 + (\tau_{co}/\sigma_{yw})^2} \tag{16a}$$

$$C_o = -0.25\, R_o\, (\sigma_{bco}/\sigma_{yw}) \tag{16b}$$

$$D_o = -0.5\left\{B_o \sin\left[\tan^{-1}(C_o\, \sigma_{yw}/\tau_{co}) + 2\varphi_{co}\right] + C_o\right\} \tag{16c}$$

φ_{co} is the optimum inclination of the tension field of subpanel "0" under combined loads*.

The shear carried by the whole panel web is thus

$$V_3 = V_{\tau o} + V_{\sigma o} + V_{\tau 1} + V_{\sigma 1}\left(\frac{\gamma_{uo} - \gamma_{c1}}{\gamma_{u1} - \gamma_{c1}}\right) \tag{17}$$

where $V_{\sigma 1}$ is the contribution of the fully developed tension field of subpanel "1" to the shear strength (Eq. (19)).

The additional stresses in the compression flange and longitudinal stiffener are indicated in Fig. 4d. They are, respectively,

$$\sigma_{f3} = \frac{(V_3 - V_2)\,\mu b}{I} y_c + \frac{H'_1}{2A_{fc}} \tag{18a}$$

and

$$\sigma_{\ell 3} = \frac{(V_3 - V_2)\,\mu b\,(y_c - b_1)}{I} + \frac{H'_1 + H''_o}{2A_{\ell s}} \tag{18b}$$

---

*φ_{co} is determined by optimizing $V_{\sigma o}$ (4).

where

$$H_o'' = V_{\sigma o} \left(\frac{\gamma_{uo} - \gamma_{c1}}{\gamma_{uo} - \gamma_{co}}\right) \cot \varphi_{co} \tag{18c}$$

and

$$H_1' = V_{\sigma 1} \left(\frac{\gamma_{uo} - \gamma_{c1}}{\gamma_{u1} - \gamma_{c1}}\right) \cot \varphi_{c} \tag{18d}$$

Stresses at the Load Developing the Post-Buckling Strength of Subpanel "1" - The tension field action contribution of subpanel "1", analogously to Eq. (14) is

$$V_{\sigma 1} = \frac{1}{2} \sigma_{t1} A_{w1} [\sin 2\varphi_{c1} - (1-\rho) \alpha_1 + (1-\rho) \alpha_1 \cos 2\varphi_{c1}] \tag{19}$$

with

$$\sigma_{t1} = \sigma_{yw} \left(D_1 + \sqrt{1 + B_1 - C_1^2 + D_1^2} \right) \tag{20}$$

where subscript "1" denotes subpanel "1". The only variable, which is different from those in Eq. (15) is

$$C_1 = 0.25 \left(\frac{y_c - b_1}{y_c}\right) \left(\frac{\sigma_{f1} + \sigma_{f2}}{\sigma_{yw}}\right) \tag{21}$$

The web strengths of both subpanels are now fully developed and the total shear is

$$V_4 = V_{\tau o} + V_{\sigma o} + V_{\tau 1} + V_{\sigma 1} \tag{22}$$

The resultant increases in the compression flange stress and the longitudinal stiffener stress are (Fig. 4e)

$$\sigma_{f4} = \frac{(V_4 - V_3)\ \mu b}{I}\ y_c + \frac{H_1''}{2A_{fc}} \tag{23a}$$

and

$$\sigma_{\ell 4} = \frac{(V_4 - V_3)\ \mu b}{I}\ (y_c - b_1) + \frac{H_1''}{2A_{\ell s}} \tag{23b}$$

where

$$H_1'' = V_{\sigma 1} \left(\frac{\gamma_{u1} - \gamma_{uo}}{\gamma_{u1} - \gamma_{c1}}\right) \cot \varphi_{c1} \tag{23c}$$

The first terms of Eqs. (23a) and (23b) are due to the bending produced by the increase in the shear force from V_3 to V_4 and the second terms are the reactions to the horizontal component of the tension field force in subpanel "1".

Stresses Due to Frame Action - The shear carrying capacity contributed by the flanges and the longitudinal stiffener is evaluated by considering a frame consisting of the flanges and the longitudinal stiffener of a typical panel as shown in Fig. 5a. It is assumed that the neighboring panels provide sufficient restraint so that the flanges and longitudinal stiffener will resist shear by the formation of plastic hinges at both ends.

The shearing force V_f, contributed by the resulting plastic mechanism, is

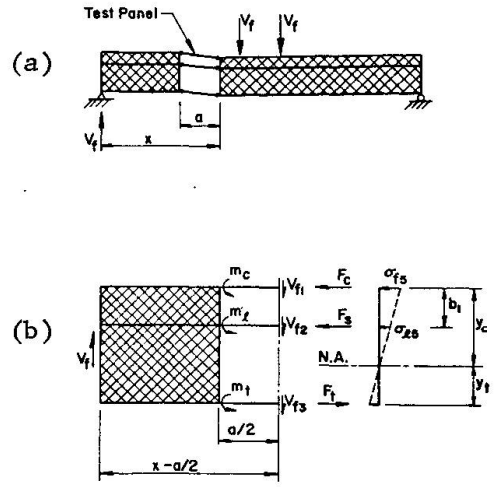

Figure 5

$$V_f = \frac{2}{a} (m_c + m_\ell + m_t) \tag{24}$$

The plastic moments m_c, m_ℓ and m_t are computed considering the axial forces and are assumed to be equal at both ends of a member.

The additional normal stresses in the flanges and stiffener are assumed to be proportional to the distance from the centroid of the girder cross section*. Moment equilibrium gives then

$$\sigma_{f5} = \frac{\mu V_f}{A_{fc} + A_{\ell s} \left(1 - \frac{b_1}{y_c}\right) \left(1 - \frac{b_1}{b}\right)} \tag{25a}$$

$$\sigma_{\ell 5} = \sigma_{f5} \left(1 - \frac{b_1}{y_c}\right) \tag{25b}$$

Critical Stresses of the Compression Flange and Longitudinal Stiffener - These critical stresses are obtained as the buckling stresses of the pin-ended columns formed by the compression flange and the longitudinal stiffener, σ_{cf} and $\sigma_{c\ell}$, respectively (1,3,5). The lateral and torsional buckling equations** given for the compression flange in Ref. 3 (Eqs. (13) and (14)) or Ref. 5 are used here also for the longitudinal stiffener with the following slenderness parameters ($\lambda = \sqrt{\sigma_y/\sigma_{cr}}$) for lateral and torsion buckling, respectively:

$$\lambda_\ell = a \sqrt{\frac{\epsilon_{ys} A_{\ell s} + 20t^2}{\pi^2 I_{\ell s}}} \tag{26a}$$

$$\lambda_t = \frac{c_s}{d_s} \sqrt{\frac{12 (1 - \nu^2) \epsilon_{ys}}{\pi^2 k_t}} \tag{26b}$$

where $k_t = 0.425$.

When the stiffener is one-sided, its critical stress $\sigma_{c\ell}$ should be obtained as that of an eccentrically loaded beam-column.

Summary of Reference Stresses - The total normal stresses introduced into the compression flange and the longitudinal stiffener are, respectively,

$$\sigma_{fs} = \sigma_{f1} + \sigma_{f2} + \sigma_{f3} + \sigma_{f4} + \sigma_{f5} \tag{27a}$$

and

$$\sigma_{\ell s} = \sigma_{\ell 1} + \sigma_{\ell 2} + \sigma_{\ell 3} + \sigma_{\ell 4} + \sigma_{\ell 5} \tag{27b}$$

*This assumption violates horizontal equilibrium, but the resultant inaccuracy is insignificant.

**Ordinary column and plate buckling equations may be used as well.

The capacities of the flange and stiffener are given by the critical stresses σ_{cf} and $\sigma_{c\ell}$, respectively.

3. ULTIMATE STRENGTH

Web or Compression Flange Failure - Depending on the relative magnitudes of the moment and shear, the capacity of a plate girder panel will usually be limited by the failure of the web plate or buckling of the compression flange. A continuous plot of the ultimate combinations of shear and moment is shown in Fig. 6.

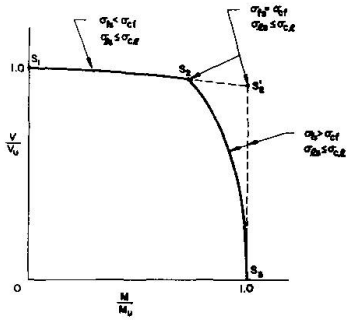

Figure 6

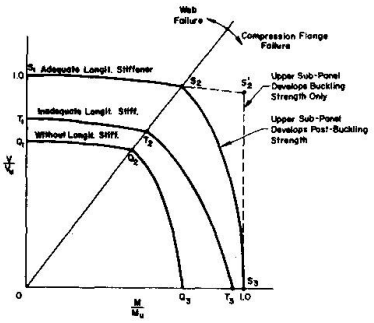

Figure 7

The failure of the web plate is typical for combinations of high shear and low moment as indicated by curve S_1-S_2 in Fig. 6. The total stresses in the flange and the longitudinal stiffener are below their critical values ($\sigma_{sf} < \sigma_{cf}$ and $\sigma_{s\ell} \leq \sigma_{c\ell}$). The subpanel webs buckle and develop their individual post-buckling strengths. With the concurrent formation of the frame action mechanism, the shear strength of the panel is then reached and is thus given by the sum of the shears from Eqs. (22) and (24)

$$V_{th} = V_4 + V_f = V_{\tau o} + V_{\sigma o} + V_{\tau 1} + V_{\sigma 1} + V_f \tag{28a}$$

The corresponding mid-panel moment is

$$M_{th} = V_{th}\, \mu b \tag{28b}$$

When the panel is subjected to a high moment, the subpanel webs will not be able to develop their full capacities before the stress in the compression flange reaches its buckling stress. The portion of the interaction curve in Fig. 6 for this case is S_2-S_3. The capacity of the panel will be given by the contribution of the web subpanels developed up to this point and a portion of the frame action. For simplicity it is assumed that the frame action shear develops in proportion to the growth of the web shear as the panel strain increases.

$$V_{th} = V_w \left(1 + \frac{V_f}{V_4}\right) \tag{29}$$

where V_w is equal to V_1, V_2, V_3, V_4 or some intermediate value corresponding to the following flange stress produced by the web forces, that is, excluding the frame action:

$$\sigma_{fw} = \frac{\sigma_{cf}}{1 + [\sigma_{f5}/(\sigma_{f1} + \sigma_{f2} + \sigma_{f3} \mp \sigma_{f4})]} \tag{30}$$

Very often the aspect ratio of subpanel "1" is greater than 3.0 and it is recommended to neglect its post-buckling strength (2,4). Then, the compression flange stress will be due to the moment only, and the interaction curve in Fig. 6 will be S_1-S_2' and S_2'-S_3. With the maximum moment capacity of the panel being

$$M_{th} = \sigma_{cf} \frac{I}{y_c} \tag{31a}$$

the shear force for S_2'-S_3 is

$$V_{th} = M_{th}/\mu b \tag{31b}$$

Tension Flange Yielding - The total stress in the tension flange due to various effects is indicated in Figs. 4b to 4e and 5b. It should not be greater than the yield stress of the flange.

Maximum Moment in Panel - Since under combined loads the moment at one end of the panel is greater than the mid-panel moment, this maximum panel moment may control the panel strength. The shear producing the maximum panel moment may not exceed

$$V_{th}' \leq \frac{M_u}{b\ (\mu + \frac{1}{2}\alpha)} \left(\frac{\sigma_{yc}}{\sigma_{cf}}\right) \tag{32}$$

A seemingly reasonable and sufficiently accurate approach, mostly on the safe side, is to keep the maximum panel moment below the moment which would produce yielding in the tension or compression flange according to the ordinary beam theory.

Panels with Inadequate Longitudinal Stiffener - When the longitudinal stiffener, subjected to the compressive force due to the panel moment and the horizontal components of the tension field forces, buckles before the panel develops its strength, the ultimate capacity of the panel will be reached in a different manner. The true failure mechanism in this case is too complicated to be analyzed at present. However, two limits of the ultimate strength are suggested here: (a) the panel develops its ultimate strength as if it had no longitudinal stiffener -- the interaction diagram is indicated by curve Q_1-Q_2-Q_3 in Fig. 7; or (b) the strength attained at the point when the longitudinal stiffener column fails -- this case is given by curve T_1-T_2-T_3 in Fig. 7. One or the other limit will give a higher value which is then to be taken as the ultimate load.

For limit (a), the ultimate strength is determined by setting b_1 and all properties of the longitudinal stiffener equal to zero, thus, leaving only the web and the flanges for computations.

For limit (b), the shear strength is given by

$$V_{th} = V_{\tau o} + V_{\sigma o}' + V_{\tau 1} + V_{\sigma 1}' + V_f \tag{33}$$

where $V_{\sigma o}'$ and $V_{\sigma 1}'$ are the incomplete tension field shears.

$$V'_{\sigma o} = \frac{2\,A_{\ell s}\left[\sigma_{c\ell} - \sigma_{\ell 5} - \frac{(V_{\tau o} + V_{\tau 1} + V'_{\sigma 1})\,\mu b}{I}(y_c - b_1)\right] - V'_{\sigma 1}\cot\varphi_{c1}}{2\,\frac{A_{\ell s}\,\mu b}{I}(y_c - b_1) + \cot\varphi_{co}} \qquad (34)$$

When the aspect ratio of subpanel "1" is greater than 3.0, as is the case for majority of plate girders, $V'_{\sigma 1}$ should be set equal to zero.

4. COMPARISON WITH TEST RESULTS

The ratio of the experimental to theoretical load is shown for twenty test results in Fig. 8. Fourteen tests on symmetrical girders are from Refs. 5 and 10 as indicated by the numbers on the dimension line in the figure. The

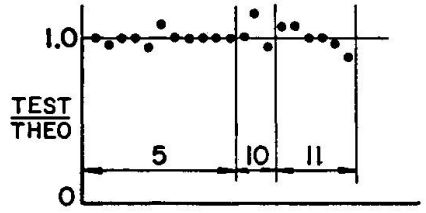

Figure 8

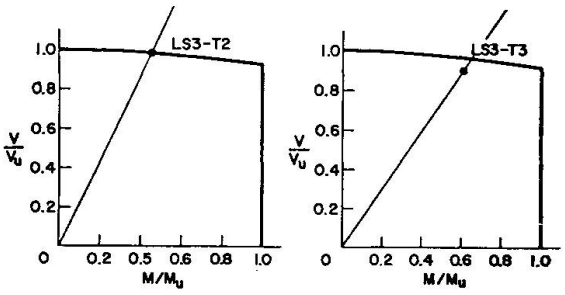

Figure 9

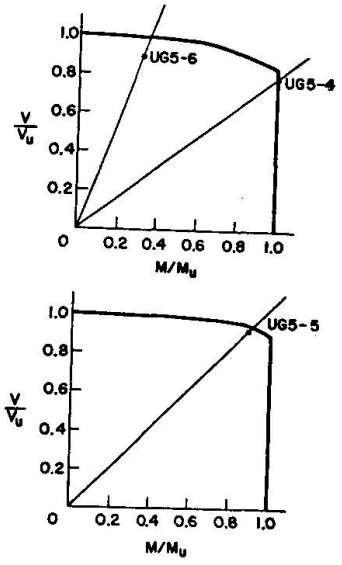

Figure 10

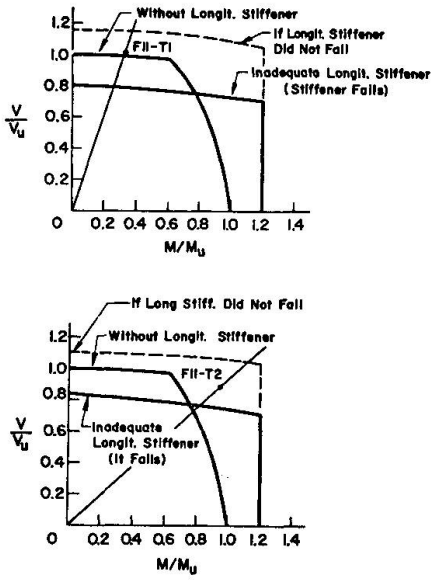

Figure 11

remaining six tests are on unsymmetrical girders from Ref. 11. The average deviation is 4%. The maximum deviation of 14% is for a panel with an inadequate longitudinal stiffener (Test F11-T2 in Fig. 11).

Interaction diagrams for two symmetrical test panels from Ref. 5 are given in Fig. 9. Three unsymmetrical panels from Ref. 11 are shown in Fig. 10. Panels UG5-6 and UG5-4 (the top sketch) were identical but were subjected to different combinations of shear and moment.

Tests on two panels with inadequate longitudinal stiffeners (Ref. 10) are compared with the proposed criteria in Fig. 11. F11-T1 is under dominant shear and its strength is essentially equal to that of a panel without the longitudinal stiffener. F11-T2 falls into the area where the two criteria have discontinuity and tend to give a too conservative prediction due to the non-utilization of the post-buckling contribution of the longitudinal stiffener.

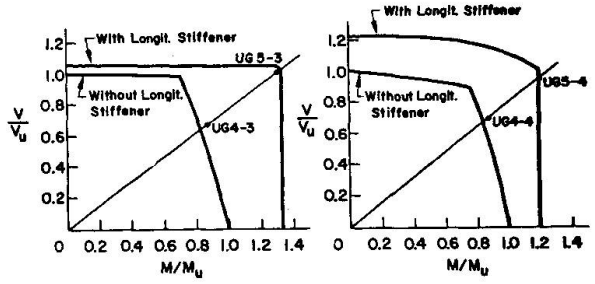

Figure 12

Two pairs of panels, one with and the other without a longitudinal stiffener, are compared in Fig. 12 (from Ref. 11). In all four panels, the capacity was limited by the strength of the compression flange. For the range of high shear and high moment, the interaction diagrams indicate a dramatic increase of the panel strength (about 44%) when the longitudinal stiffener is introduced into the panel.

5. CONCLUDING REMARKS

The following conclusions can be drawn from this investigation:

1) The interaction curve between moment and shear consists of two portions: web failure which occurs under dominant shear and flange failure which occurs under dominant moment.

2) The panel strength for the web failure mode may be computed as a sum of the shear strengths of the individual web subpanels (buckling and post-buckling strengths) and the capacity of the plastic mechanism formed by the flanges and longitudinal stiffener (frame action).

3) The force in a flange for the flange failure mode has contributions from the bending moment and a component of the force due to a partially developed tension field.

4) When the longitudinal stiffener is inadequate, the failure load may be conservatively assumed to be the higher one of the following: (a) the ultimate strength of the panel as if it had no longitudinal stiffener or (b) the strength developed by the panel at the point when the longitudinal stiffener column fails.

5) A comparison of the theory with the results of twenty tests gives an average correlation of 4%. Thus, the presented theory provides a reliable

means of determining the static ultimate strength of longitudinally stiffened steel plate girder panels subjected to shear, bending, or a combination of shear and bending.

6) In application, the method requires some iterative operations and, thus, is not readily suitable for manual calculations. However, the numerical computer output of a program based on the method can be used to develop simple design formulas. Such a development was very successful for transversely stiffened plate girders (9).

Among many aspects of the behavior of longitudinally stiffened plate girders which need further investigation are the following:

1) Tests on composite girders are needed to check whether the proposed approach is applicable to them since the concrete slab acting together with the top girder flange may make a greater contribution to the girder strength than given by the frame action.

2) More work is needed to establish design criteria for transverse stiffeners.

REFERENCES.

1. Basler, K., and Thürlimann, B., "Strength of Plate Girders in Bending", J. ASCE, Vol. 87 (ST6), Aug. 1961.

2. Chern, C., and Ostapenko, A., "Ultimate Strength of Plate Girders under Shear", Fritz Engrg. Lab. Rept. No. 328.7, Lehigh Univ., Aug. 1969.

3. Chern, C., and Ostapenko, A., "Bending Strength of Unsymmetrical Plate Girders", Fritz Engrg. Lab. Rept. No. 328.8, Lehigh Univ., Sept. 1970.

4. Chern, C., and Ostapenko, A., "Unsymmetrical Plate Girders under Shear and Moment", Fritz Engrg. Lab. Rept. No. 328.9, Lehigh Univ., Oct. 1970.

5. Cooper, P. B., "Strength of Longitudinally Stiffened Plate Girders", J. ASCE, Vol. 93 (ST2), Apr. 1967.

6. Kollbrunner, C. F., and Meister, M., "Ausbeulen", Springer-Verlag, Berlin, 1958.

7. Ostapenko, A. and Chern, C., "Strength of Longitudinally Stiffened Plate Girders", Fritz Engrg. Lab. Rept. No. 328.10, Lehigh Univ., Dec. 1970.

8. Ostapenko, A., Yen, B. T., and Beedle, L. S., "Research on Plate Girders at Lehigh University", Final Report, 8th IABSE Congress held in New York, Sept. 1968, IABSE, Zurich.

9. Ostapenko, A., Chern, C., and Parsanejad, S., "Ultimate Strength Design of Plate Girders", Proc. of the Conference on Developments in Bridge Design and Construction, held in Cardiff, Apr. 1971. To be published by Crosby Lockwood & Son, Ltd., London, Nov. 1971.

10. Patterson, P. J., Corrado, J. A., Huang, J. S., and Yen, B. T., "Fatigue and Static Tests on Two Welded Plate Girders", WRC Bulletin 155, New York, Oct. 1970.

11. Schueller, W., and Ostapenko, A., "Tests on a Transversely Stiffened and on a Longitudinally Stiffened Unsymmetrical Plate Girder", WRC Bulletin 156, New York, Nov. 1970.

NOTATION

In general, subscripts "1" and "0" refer to subpanels "1" and "0", respectively. Subscript "y" means yielding, "u" - ultimate, "f" - compression flange, "w" - web. Definition is given here only for the symbols which are not in common usage and are not defined in the text or in the figures.

A_{fc} area of the compression flange

$A_{\ell s}$ area of the longitudinal stiffener = $2c_s \times d_s$ for a two-sided stiffener

$I_{\ell s}$ moment of inertia of the longitudinal stiffener about the vertical axis of the girder cross section

c_s width of the longitudinal stiffener on each side

d_s thickness of the longitudinal stiffener

ε_{ys} yield strain of the longitudinal stiffener

ρ averaging coefficient of the tension field stress in the elastic triangular portions; it is assumed to be equal to 0.5 for ordinary welded steel girders

φ_c optimum inclination of the tension field force in a panel under combined loads

SUMMARY

The static ultimate strength of longitudinally stiffened plate girder panels subjected to any combination of shear and bending is determined for symmetrical, unsymmetrical, homogeneous and hybrid girders. The panel strength is obtained as a sum of the ultimate strengths of the two web subpanels and of a frame formed by the flanges and the longitudinal stiffener. The average deviation of the theory from test results is 4%.

RESUME

Les auteurs déterminent la charge de ruine statique des poutres à âme pleine munies de raidisseurs longitudinaux, soumises à une combinaison quelconque de flexion et de cisaillement; la méthode s'applique aux poutres symétriques, asymétriques, homogènes et hybrides. La charge de ruine d'un panneau se compose de la résistance limite des deux sous-panneaux d'âme et de celle du cadre formé par les membrures et le raidisseur longitudinal. La différence moyenne entre la théorie et les essais atteint 4 %.

ZUSAMMENFASSUNG

Die Traglast statisch belasteter längsversteifter Blechträger unter Biegung und Querkraft wird bestimmt. Die Methode ist für symmetrische und unsymmetrische Träger anwendbar, die aus einer oder mehreren Stahlgüten zusammengeschweisst sein können. Die Gesamttraglast setzt sich aus den Tragfähigkeiten der zwei von der Längssteife gebildeten Stegfeldern und des aus den Flanschen und der Längssteife geformten Rahmens zusammen. Die durchschnittliche Abweichung der theoretischen Ergebnisse von den experimentellen beträgt 4%.

Leere Seite
Blank page
Page vide